Swedish University of Agricultural Sciences
Faculty of Veterinary Medicine and Animal Science

Algorithms offering kinetic analysis of drug induced proteasome inhibition and cell clump formation from time lapsed microscopy

Muhammad Kashif

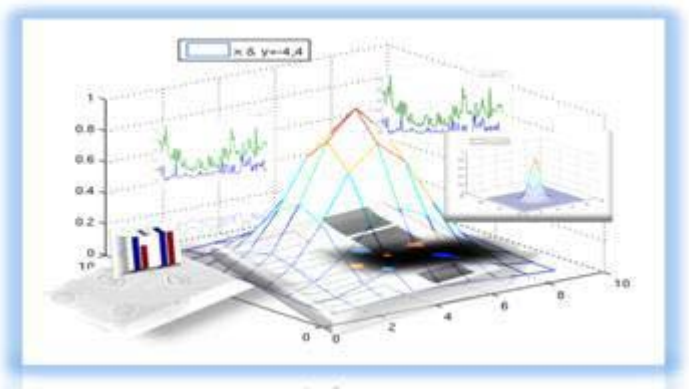

Department of Animal Breeding and Genetics
Examensarbete 326
Uppsala 2010

Master's Thesis, 30 HEC

One-Year Master's Programme in Biology – Bioinformatics

Swedish University of Agricultural Sciences
Faculty of Veterinary Medicine and Animal Science
Department of Animal Breeding and Genetics

Algorithms offering kinetic analysis of drug induced proteasome inhibition and cell clump formation from time lapsed microscopy

Muhammad Kashif

Supervisors:
Mats Gustafsson, UU, Cancer pharmacology & informatics
Erik Bongcam-Rudloff, SLU, Department of Animal Breeding and Genetics
Examiner:
Rolf Larsson, UU, Cancer pharmacology & informatics

Credits: 30 HEC
Course title: Degree project in Animal Science
Course code: BI1021
Programme: One-Year Master's Programme in Biology
- Bioinformatics

Level: Advanced, A2E

Place of publication: Uppsala
Year of publication: 2010
Cover picture: Muhammad Kashif
Name of series: Examensarbete 326
Department of Animal Breeding and Genetics, SLU
On-line publication: http://epsilon.slu.se

Key words: Image processing; time lapsed microscopy; kinetic studies; cell clumps; proteasome inhibition

CONTENTS

ABSTRACT

High content screening (HCS) has potential to transform many biological fields, ranging from drug discovery to gene function discovery. HCS with time lapsed microscopy provide valuable insight information about live cells experiments that are usually lost during manual end point experiments. By means of novel bioinformatics algorithms, huge amount of phenotypic data might become available by these techniques which can be used to understand effects of chemical compounds on the cells and profile phenotypically both cell line and chemical compounds. The resultant data can also be compared with other experiments to find out the efficiency and affectivity of the different compounds under same conditions. Recent results also demonstrate that phenotypic profiles can be used to infer specific gene perturbations.

In this thesis, novel algorithms for such phenotypic profiling were implemented and demonstrated to be very useful revealing unknown kinetic information regarding two proteasome inhibitors (Bortezomib and CB3) as well as about cell clump formation during cell line growth on honeycomb nanoculture plates. The novel algorithms include specialized solutions both for phase contrast microscopy and fluorescent microscopy and are based on the publicly available cell image processing package Cell Profiler from Broad Institute.

1. INTRODUCTION

In conventional biomedical drug and toxin exposure experiments, in which cell cultures are treated for many hours or even days, information about the resulting effects are usually obtained only at the end of experiment. As a result, potentially valuable kinetic information about the drug/toxin effects on the cell cultures is lost. Time lapse microscopy [36] provides a promising way to capture the kinetic details of the drug induced effects. As these microscopes provide information in the form of images, it is nontrivial to extract useful quantitative information from them. For example, it is almost impossible, or by any measures exhausting and time consuming, to manually count the cells and their features manually (with naked eye).

To handle this situation high content screening (HCS) comes into play. HCS can be defined as "use of spatially or temporally resolved methods to discover more in an individual experiment than one single experimental value" [16]. Thus HCS may be broadly defined as automated methods for rapid and quantitative (high content) analysis of data, usually images. In HCS, images obtained from live cell microscopy are fed to image analysis software that extracts phenotypic information. This phenotypic information usually comes in bulk and can be analyzed to extract different features to draw different conclusion. Usually this information is fed to software that analyzes the required feature(s) and performs the phenotypic profiling or provides the pharmacological control results. This novel information can be used in various fields of biomedicine, for example in the processes of drug discovery, gene prediction and prediction of their functions.

Time lapsed microscopy could be based on different imaging modalities such as phase contrast or fluorescent microscopy. Phase contrast microscopy produces the images on the basis of changes in phase shift. It does not require the treatment of the sample with any dye or protein. While the basic principle of fluorescent microscopy is to introduce fluorescent molecules inside the cells

which then are traced due to fluorescent signals. Using these kinds of microscopic techniques one can analyze the cellular and sub cellular structures and can compare them with the results of other experiments.

The HCS data sets used in this thesis to demonstrate the great potential of the novel algorithms developed came from the MelJuSo-Ub cell line treated with Bortezomib and CB3. Bortezomib is an anti cancerous drug having role in proteasome inhibition. This is the first proteasome inhibition drug that is going to be tested in humans, especially for multiple myeloma. CB3 is a novel proteasome inhibition anti cancerous hit and is still in the process of drug discovery. Another dataset used to demonstrate the potential came from the cell clumps experiments where two different cell lines, HCT 116 and hTRET RPE-1, were monitored with respect to their cell clump formation during their growth. The cell lines were phenotypically profiled in terms of features like, intensity, size of clumps, shape of the clumps and number of clumps etc.

The development of the novel bioinformatic algorithms consisted of two different parts. The first part concerned developing a successful pipeline of processing steps for information extraction from phase contrast cell images using CellProfiler, an open source image processing package from Broad Institute (USA). This involved the usage of most suitable edge detection algorithm and then feeding edged images to segmentation modules for object identification and information extraction. The second part considered development of successful information extraction from fluorescent images. The proper usage of amplitude thresholding to discriminate between objects and background is a key here.

A schematic diagram of the above mentioned procedure is shown in fig.1.

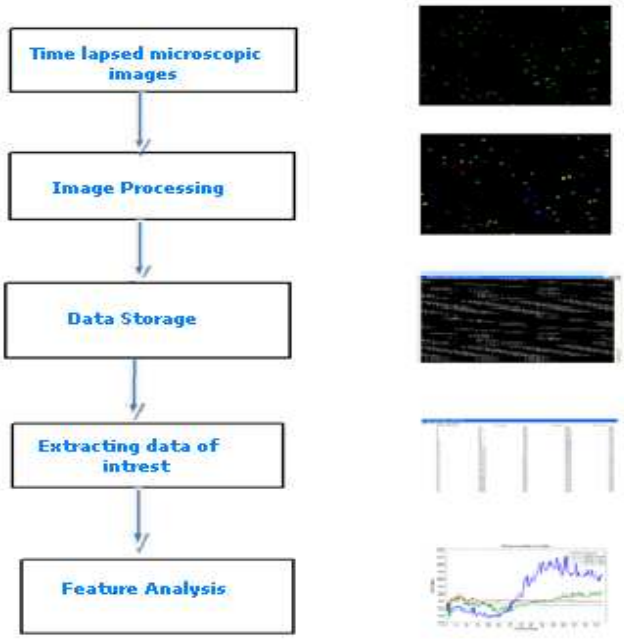

Fig.1. Procedure for phenotypic feature extraction and analysis from time lapsed microscopic images (phase contrast + fluorescent) obtained from Incucyte™ and IncucyteFLR. Time lapse microscopic images were input to the tailored image processing software. The resultant data after image processing was stored in database and data which was related to feature of interest was extracted for further analysis.

The rest of this thesis is organized as follows. In section 2, brief backgrounds are offered to some of the most central topics and methods used in the thesis project reported here. In section 3, the main aims of the thesis project are presented. In section 4, a more technical and formal description of the specific materials and methods used, including parameter settings, are described. In section 5, the results of the bioinformatics analyses performed are presented. Finally, section 6 provides a general discussion and suggestions for future work.

2. BACKGROUND

This thesis is covering a broad range of different topics. In order to make it self contained, in this section brief introduction to the most central methods and ideas are presented.

2.1. Phase Contrast Microscopy

Phase contrast microscopy has been used since 1942 in microscopy, when F.Zernike [1][2] successfully applied it for observation of transparent objects. The basic idea here is that when light passes through transparent object, small phase shifts in the light are observed. These phase shifts are converted to contrast changes in the image. The advantage of this technique lies in observing the cells without modifying them. Many cells or cell parts (bacteria, tails of sperms etc) are transparent and invisible unless stained. However phase contrast microscope can detect them due to changes in their composition and densities. It also makes it possible to observe living cells and their life cycles. It does not require staining of cells thus enabling researchers to observe the unmodified cells rapidly and cheaply. The main disadvantage [3] of this technique is the halo around the edges of the object and black & white nature of the image.

2.2 Fluorescent Microscopy

Biological pathways can be observed if a protein specific to them can be labeled and located in the live cell environment, indeed this type of observations are not possible with phase contrast microscopy. Fluorescence is a phenomenon occurring when a molecule being excited via illumination at one specific wavelength is reemitting light at some other wavelength [5]. To employ this phenomenon in cell imaging, part/ parts of the cells which are of interest are dyed or fluorescent protein is attached; and resultant colors are imaged/ observed for analysis.

Fluorescent microscopy brought great advantages for biologists they can now observe sub cellular components. They can also visualize cellular processes and when coupled it with time lapse microscopy it let them to understand cellular dynamics. Limitations of fluorescent microscopy basically lie in that fluorescent probes can affect the cellular function and structure and that it might be very difficult to transfect or by other means insert the fluorescent probe inside the cell. It also requires the deposition of some energy during the excitation phase of fluorescence process.

2.2.1 Fluorescent Techniques

Researchers can detect objects of interest inside the cells by using fluorescent techniques. Fluorescent probes can detect components of interest in complex bimolecular systems with

selectivity and sensitivity. The process of fluorescence consists of three stages [7] in a molecule called fluorophore.

Stage 1. Excitation: In this stage fluorophore is provided with a photon of energy as a result of it an excited electronic state is created.

Stage 2. Excited State Life Time: This excited state of the fluorophore is usually 1-10 nanoseconds. During which two types of the changes can occur. Firstly the energy of the fluorophore at the excited electronic state can dissipate, resulting in the creation of relaxed excited state. This stage can further dissipate the energy to originate fluorescence emission stage. Secondly, some of the fluorophore at the excited electronic state emits the fluorescence and return directly back to ground state.

Stage 3. Fluorescence Emission: A photon is emitted from the fluorophore bringing it back to ground state from the excited state. The energy of the emitted photon can be decreased due to the energy dissipation at the stage2 mentioned above.

The process of the fluorescence emission is cyclic in nature, thus a fluorophore can be excited and detected repeatedly. Unless it is destroyed at the excited state.

2.2.2 History

Fluorescent microscopy may be traced back to 1873 when Ernst Abbe [6] provided a microscope for biologists although it had many problems like spherical aberrations etc. In 1903 Henry Friedrich invented ultra-microscope to observe colloids as bright spot of light [6].Further advances in the field of fluorescent microscopy led to the invention of light fluorescent microscope in 1948 [6]. Discovery of laser also had its impact on microscopy and laser based microscope was invented in 1982 by Carl Zeisses [6]. A great advancement in this filed has also been made since the discovery of green fluorescent protein in 1994**.**

Immunofluorescence techniques and covalent bonding was being used for fluorescent techniques in 90s [5]. The main breakthrough in this field came with the discovery of green fluorescent protein (GFP). GFP was extracted and reported in 1962 [8] but its ability to be used as gene expression marker remain hidden until 1994 when ChalfieM et al [9] reported the use of GFP as marker of gene expression. Since then many variant of GFP have also been reported such as cyan fluorescent protein and yellow fluorescent protein etc.

2.3 Incubators for Live Cell Imaging

Incubators are the devices which are used to grow and maintain the cells in controlled environment outside the body. With the development of above mentioned techniques there was need to study the cells automatically in incubators. Various companies started developing incubators such as RS Biotech, Prodigy biosystems, Essen Biosciences etc.

Essen Biosciences [10] used these basic principles of phase contrast/ fluorescent microscopy along with live cell imaging over the time in a controlled environment to develop the Essen Incucyte. Previously one had to grow the cells in the incubator and then take them to the

microscope for imaging after a specific time interval to observe the features of interest. During this shifting from incubator to microscope the environmental conditions may be hampered and the process is labor intensive. Essen Incucyte solves this problem by embedding microscope within the incubator. Now live cells can be observed/imaged over long time periods without affecting them and their kinetic studies become convenient. Four different models of Incucyte models are available. These are:

- ***Incucyte™***
  This is the machine that was the first one of this line of product from Essen Biosciences. It can image sample on the basis of phase contrast microscopy and is unable to produce color images. Thus one has to analyze the fluorescent assays on the basis of gray scale rather than color images. It is compatible to Microsoft platform and works in the temperature interval from 0 to 33°C.

- ***Incucyte HD***
  It is quite similar to Incucyte™. The difference lies in its imaging technique. Instead of phase contrast microscopy another technique called high definition (HD) imaging mode is used. This method is developed by Essen to improve the performance phase contrast imaging especially to handle the aberrations caused by fluid meniscus in 96- and 384- well plates. It is compatible to Microsoft plate form and its environmental controller works in the temperature interval from 0 to 33°C.Incucyte HD cannot produce the color images and can provide zooming up to 20x.

- ***IncucyteFLR***
  This version of Incucyte has a fluorescent microscope in addition to retaining all the features of the Incucyte™ and Incucyte HD. With the ability to handle the fluorescent assays this version of Incucyte enable researchers to handle the GFP or antibodies based assays. In addition to it a kit is provided that allow researchers to compare the fluorescent values of different experiments. IncucyteFLR is compatible to Microsoft windows plate form. The temperature interval that is required for operating environmental controller is 0 to 33°C.

- ***Incucyte EX***
  This version is quite different from other versions of Incucyte. It is designed to function outside the incubator. It can be used for live cell imaging to third party cell culture system. It provides the around the clock and robot controlled collection of images along with retrievals. It does not have fluorescent microscope. Incucyte EX can work with Microsoft Windows XP, Microsoft Windows Vista and Windows 7. It can produce the JPEG and TIFF images.

2.4 Image Processing Software

With the usage of time lapsed microscopy, the number of the images that are produced during biological experiments (RNAi reagents etc) are increasing rapidly. But the problem arises at the end of getting useful quantitative information from these images as it is difficult and tedious to characterize them manually (with eye).These difficulties rapidly increase when/of the whole

spectrum of information (intensity of fluorescent signal, size of cell and nucleus etc) is of interest. Here comes the role of the image processing in as a technology of great importance.

A number of cell image processing open source software are available [11, 12] such as CellProfiler, BioimageXD and ImageJ etc. These can be used as per specific needs of the research or tasks. CellProfiler [13] is an open source image processing software that was developed by BROAD institute [14] in 2006.The beauty of this software lies in its modular approach. One can develop a tailor made image processing pipeline instead of using the whole software package and it is applicable [15] both for mammalian and non-mammalian cells. This software has modules suitable for measuring the size, shape, solidity, area, intensity of signal of not only cells but also the sub-cellular structures in high throughput manner. Here solidity is calculated as convexity which means only non-hallow parts of objects are considered in this calculation and is actually the proportion of the pixels in the convex hull and object. Therefore solidity provides the important insight about the object that how much of its area is solid. In addition to its basic features, image correction functions such as illumination correction are also provided. CellProfiler is coupled with the subsequent companion software package CellProfilerAnalyst that can be used to analyze the data extracted by CellProfiler. The role of edge detection algorithms and threshold detection techniques is paramount in this software.

2.5 Image Processing Algorithms

Edge detection is central in image processing and is very important for identification and classification of objects. CellProfiler uses edge detection algorithms designed especially for phase contrast images. The detection of edges is usually the exploitation of the property that the intensity at the edges has abrupt changes. If a pixel shows an abrupt change of intensity as compare to neighbors then it can be classified as edge [24] [25]. Edge detection itself is a vast field in image processing and has a number of methods. In summary, there is a large body of alternative methods for edge detection and background and object separation. Here follows a short review.

2.5.1 Edge detection methods

Sobel is an edge detection method that performs spatial gradient measurements on the image of interest to find out high spatial frequency that is considered as edge [26]. Gradient measurement is very effective in edge detection as Prewitt algorithm also uses this property. It measures the horizontal and vertical gradient of input image. The both gradients are then combined and threshold is applied to detect edges [27]. Canny algorithm uses a step approach in addition to edge detection for optimal edge detection. In first step noise of the image is reduced by applying a Gaussian filter. Then image intensity gradient is found by applying an edge detection method. The next step is to find local maximum in the direction of gradient that leads to the last step of thresholding [28] and as a result of the whole process every pixels of an image will be classified as edged or non-edged.

Another optimal algorithm that can be used of edge detection is based on the Laplacian (divergence of gradient) of a bi-variate Gaussian function [29].Another common strategy is to apply one or several smoothing filters and then calculate the ratio of the resultant images to find the edges [30].

2.5.2 Boundary closing methods

In addition to above mentioned algorithms which can identify the edges in disconnected form there are those algorithms that can close the boundaries of the objects in order to separate the objects from the background. Otsu algorithm is one such type of algorithm that makes the histogram of intensities and divides the image into classes of pixels. The threshold intensity used minimizes the variance in the classes [31]. In case of dark and dominant background images, the background- symmetric algorithm is often useful [32]. It is a thresholding and histogram based algorithm. This algorithm tries to find asymmetric distinct dominant peak as the background by searching for the maximum value in the histogram [33].

2.5.3 Other

Ridler and Calvard proposed a methodology for low contrast and handwritten images. They proposed an iterative technique to calculate thresholding level successively. The samples of background were taken closer and closer to the object after every iteration [34]. Difference of Gaussian (DoG) algorithm provides another way of edge detection in which original image in blurred by using Gaussian filter and this process is done twice. Then one blurred image is subtracted from another less blurred image that produced the sharpen edges and noise in the image is reduced [35].

2.6 High Content Screening & Role in Drug Discovery

HCS is an excellent method for drug discovery and based on a combination of chemistry, biology, microscopy, image processing and analysis for high throughput automated research. The history of HCS can be traced back to 1950 with development of cytometry when Coons and Kaplan [17] developed immunoflourescence microscopy. The instrumentation and imaging software [19, 20, 21] come in to lime light in late 1960s and in 1970s [18]. Video microscopy [22] started to mark its importance in 1980s when efforts were made to enhance the contrast of fluorescence. GFP in 1994 revolutionized this field and pave the way for making HCS popular.

HCS is being applied in pharmaceutical industry for R&D [23]. With the help of high content assays the rate of failure of drug candidates in the later stages of drug development can be reduced, because compound toxicity and efficacy can be more successfully predicted at earlier stages of the drug development. HCS has also opened new areas in drug discovery because it can handle multiplexing assays [18]. Single or combined compounds can be tested against the various cellular functions such as apoptosis, proteasome inhibition etc. These can lead to the drug discovery of new more effective compounds in the less time.

2.7 Kinetic Studies of Cell Cultures

Cell kinetics is the studies of the time parameter based measurement in the biological systems [51]. They are very helpful in understanding tumor growth and phenotypic changes with the passage of time. Kinetic studies are very important in case of drug activity analysis as in contrast to the end point analysis, it can provide lot of information how drug effected as a function of time. Gene functions can also be studied in great detail with the help of kinetic phenotypic studies of cellular and sub cellular organelles [37].Insight kinetic analyses of these experiments can be helpful in better understanding of effect of certain compound on the cells and can help in drug discovery.

3. AIMS OF STUDY

The aims of this thesis project may be divided into bioinformatic aims and biomedical aims to stress the fact that the project is inter-disciplinary but with a strong emphasis on the bioinformatic part.

The main (bioinformatic) aim of this thesis project was to develop, implement and demonstrate a bioinformatic infrastructure, including novel algorithms, which are able to offer kinetic analyses of drug induced effects from time lapsed microscopy. The bioinformatics infrastructure developed should be generic enough to become useful in a broad range of biomedical projects yet specific enough to offer a feasibility study in cancer pharmacology before initiating such type of experiments on large scale.

The main biomedical aim of this project was to contribute to an improved kinetic understanding of drug induced proteasome inhibition in cancer cell lines. The second main biomedical aim was to offer a first quantitative analysis of the phenomenon of spontaneous cell clump formation.

More specifically, the aims of this project were:

- Establish one or several analytic pipelines for kinetic phenotyping of growing cell populations.
- Demonstrate the biomedical potential of such analytic pipelines by applying them to time lapsed microscopy data collected from at least three different cell lines using at least two different drugs.

4. MATERIALS & METHODS

In this section, a quite formal presentation of the materials and methods employed, including parameter settings, are briefly described.

4.1 Work flow

Phase contrast and fluorescent time lapsed microscopic images were obtained from Incucyte^{TM} and IncucyteFLR respectively. In case where images have high background noise; they were smoothed by applying the Gaussian filter. Then these images were input to the image processing software CellProfiler as shown in fig 1. Here various pipelines were developed and tested for successful extraction of features from whole set of images. Once successful pipeline was developed, set of images (~145 for each analysis in our case) were processed with same pipeline. Result of image processing was numeric data that was stored in the MySql 5.1 database as shown in the step 3 of the fig 1. Now data can be queried (by structured query language) and desired features can be manipulated and extracted from data base. Data was extracted usually in the form of the text files which were in turn fed to Matlab 7.9 for analysis.

4.2 Proteasome inhibition analysis

4.2.1 Instrument

IncucyteFLR was used for the fluorescent time lapsed microscopy and Incucyte™ was used for phase contrast time lapsed microscopy.

4.2.2 Cell Line

MelJuSo-Ub human melanoma cell line was used in these experiments. This cell line was fluorescently labeled with yellow fluorescent protein.

4.2.3 Compounds

Cell line was treated with Bortezomib and CB3. Bortezomib is the first compound which is in the clinical trial phase for treatment of cancer in human while the CB3 is the new hit found at Deptt. of Clinical Pharmacology, Uppsala University.

4.2.4 Duration of experiment

The cells were placed inside the IncucyteFLR for 75 hrs in case of fluorescent probe, and were placed for 75 hrs in side Incucyte™ in case of Phase contrast probe.

4.2.5 Interval of imaging

The treated cells were imaged after every 30mins inside both IncucyteFLR and Incucyte™.

4.2.6 Software

CellProfiler version 1.0 was used for processing of acquired phase contrast images from Incucyte™ while CellProfiler version 2.0 was used to for fluorescent images from IncucyteFLR. These images were processed to extract desired features i-e number, size, area, intensity and shape of cells.

Two different pipelines were developed, each for fluorescent and phase contrast images. As shown in table 1 and table 2 respectively.

Table 1 *Pipeline in detail for Bortezomib, CB3 and control fluorescent images.*

Module Name	Parameter Name	Value
LoadImages	File type to be loaded	Individual images
	File selection method	Text-Exact match
	Text that these images have	.jpg
	Name this loaded image	BR_CB_CN
ColorToGray	Select the input image	BR_CB_CN
	Conversion method	Combine
	Name the output image	GrayCmb_BR_CB_CN
IdentifyPrimaryObjects	Select the input image	GrayCmb_BR_CB_CN
	Name the primary objects	Cell_BR_CB_CN
	Select the thresholding	Background Global
	Method to distinguish clumps	Intensity
	Typical diameter of objects	Calculate and specify for

		your own images
MeasureObjectIntensity	Select the image to measure Select the object to measure	GrayCmb_BR_CB_CN Cell_BR_CB_CN
MeasureObjectSizeShape	Select the objects to measure Calculate Zernike features	Cell_BR_CB_CN False
ConvertObjectsToImage	Select the input image Select the color map Select the color type	Cell_BR_CB_CN Default Color
SaveImages	Select the file format to use Select how often to save	Bmp Every cycle
ConserveMemory	Specify which images Images to remove	Images to remove Cell_BR_CB_CN, GrayCmb_BR_CB_CN
ExportToSpreadsheet	Select or enter the column Export all measurements	Tab True
ExportToDatabase	Database type DatabaseName User name & password	MySql Db_Bor_CB3_Cnt Enter your own user name & password

Table 2 *Pipeline in detail for Bortezomib, CB3 and control phase contrast images.*

Module Name	Parameter Name	Value
LoadImages	How do you want to load these files What type of files you are loading Text that these images have Name of loaded image in CellProfiler	Text-Exact match Individual images .tif P_BR_CB_CN
ColorToGray	Select the input image Conversion method Name the output image	P_BR_CB_CN Combine GrayCmb P_BR_CB_CN
FindEdges	Threshold adjustment factor Edge finding method Name of image with edge identified	1 Ratio Edged_P_BR_CB_CN
IdentifyPrimAutomatic	Select the input image Name the primary objects Select the thresholding Method to distinguish clumps Typical diameter of objects	Edged_P_BR_CB_CN Cell_P_BR_CB_CN Robust Background Global Shape Calculate and specify for your own images
MeasureObjectIntensity	Select the image to measure Select the object to	GrayCmb P_BR_CB_CN Cell_P_BR_CB_CN

	measure	
MeasureObjectAreaShape	Select the objects to measure	Cell_P_BR_CB_CN
	Calculate Zernike features	No
SpeedUpCellProfiler	Do you want to clear the memory	Yes
	Image to remain in memory	Do not use
ExportToDatabase	Database type	MySql
	DatabaseName	Db_Phase_Bor_CB3_Cnt

4.2.7 Database

MySql 5.1 open source database was used to store the information after processing images.

4.2.8 Programming language

The stored data is analyzed by developing graphs of different variables with help of Matlab 7.9.0.

4.3 Cell Clumps Formation Analysis

4.3.1 Instrument

Instrument that was used for this analysis was Incucyte^{TM}, only phase contrast images were available for analysis. Cells were grown on nanoculture plates. A thin film was added on the bottom of these plates having honeycomb pattern.

4.3.2 Cell Line

Two cell lines hTERT RPE-1 and HCT116 were used. hTERT RPE-1 cell line is eye retina pigmented epithelium cells that form small spheroids, while HCT116 is colon carcinoma cell line and form the large spheroids.

4.3.3 Stimulus

The cell lines were untreated. The experiment aimed to grow the cells on nanoculture plates that is completely new technique.

4.3.4 Duration of experiment

The cell lines were placed inside the Incucyte^{TM} for 75 hrs where they were imaged after every 30mins.

4.3.5 Background suppression using Gaussian filter

The background noise was produced in the images due to nature of nanoculture plates and film patterns. The background was suppressed by the use of the Gaussian filter. For each pixel in the original image, the Gaussian filter is replacing the current pixel value by a weighted sum of pixel values. The weight w (i,j) for pixel (i,j), relative to the current pixel, is given by

$$w(_{i,j}) = b^{-x*i^2-y*j^2}$$

Where i and j are integers and where b, x and y are user defined parameters.

Thus, the weight for the current pixel itself is w (0,0)=b, and for its closest neighbor in the x-direction, the weight is w(1,0)=b*exp(-x), etc. The two different parameter settings for b, x and y used in the analyses are presented in Table 3.

Table 3 *Value of parameters (number of pixels that will be averaged) for dark and light images for images of both cell lines*

hTERT RPE-1 images		**HCT116 images**	
Dark images	**Light Images**	**Dark Images**	**Light images**
x= -4, y=4, b=0.2	x=-1, y=1, b=0.2	x=-10, y=10, b=0.2	x=-2, y=2, b=0.2

4.3.6 Software

CellProfiler Version 2.0 was used for processing of the filtered images. The images were processed to extract the following features: number, size, area, intensity and shape of cells, respectively.

Two different pipelines were developed, one for hTERT RPE-1 and one for HCT 116 cell line images. As shown in table 4 and table 5 respectively.

Table 4 *Pipeline in detail for hTERT RPE-1clumps phase contrast images.*

Module Name	**Parameter Name**	**Value**
LoadImages	File type to be loaded	Individual images
	File selection method	Text-Exact match
	Text that these images have	.jpg
	Name this loaded image	hTERT_RPE-1
ColorToGray	Select the input image	hTERT_RPE-1
	Conversion method	Combine
	Name the output image	Gray_hTERT_RPE-1
EnhanceEdges	Select input image	Gray_hTERT_RPE-1
	Select edge finding method	Sobel
	Select edge direction to	All
	Name output image	Edged_hTERT_RPE-1
IdentifyPrimaryObjects	Select the input image	Edged_ hTERT_RPE-1
	Name the primary objects	Spheroid_ hTERT_RPE-1
	Select the thresholding	Background Global
	Method to distinguish clumps	None
	Typical diameter of objects	30-240
MeasureObjectIntensity	Select the image to measure	Gray_hTERT_RPE-1
	Select the object to measure	Spheroid_ hTERT_RPE-1
MeasureObjectSizeShape	Select the objects to measure	Spheroid_ hTERT_RPE-1
	Calculate Zernike features	False
MeasureImageAreaOccupied	Select Object to measure	Spheroid_ hTERT_RPE-1
ConvertObjectsToImage	Select the input image	Spheroid_ hTERT_RPE-1

	Select the color map Select the color type	Default Color
SaveImages	Select the file format to use Select how often to save	Bmp Every cycle
ConserveMemory	Specify which images Images to remove	Images to remove Spheroid_hTERT_RPE-1Edged_ hTERT_RPE-1
ExportToSpreadsheet	Select or enter the column Export all measurements	Tab True
ExportToDatabase	Database type DatabaseName User name & password	MySql Db_hTERT_RPE-1 Enter your own user name & password

Table 5 *Pipeline in detail for HCT 116 clumps phase contrast images.*

Module Name	Parameter Name	Value
LoadImages	File type to be loaded File selection method Text that these images have Name this loaded image	Individual images Text-Exact match .jpg HCT_116
ColorToGray	Select the input image Conversion method Name the output image	HCT_116 Combine Gray_ HCT_116
EnhanceEdges	Select input image	Gray_ HCT_116
	Select edge finding method	Sobel
	Select edge direction to	All
	Name output image	Edged_ HCT_116
IdentifyPrimaryObjects	Select the input image Name the primary objects Select the thresholding Method to distinguish clumps Typical diameter of objects	Edged_ HCT_116 Spheroid_ HCT_116 Ridler Calvard Global None 25-310
MeasureObjectIntensity	Select the image to measure Select the object to measure	Gray_ HCT_116 Spheroid_ HCT_116
MeasureObjectSizeShape	Select the objects to measure Calculate Zernike features	Spheroid_ HCT_116 False
MeasureImageAreaOccupied	Select Object to measure	Spheroid_ HCT_116
ConvertObjectsToImage	Select the input image Select the color map Select the color type	Spheroid_ HCT_116 Default Color
SaveImages	Select the file format to	Bmp

	use Select how often to save	 Every cycle
ConserveMemory	Specify which images Images to remove	Images to remove Spheroid_HCT_116Edged_ HCT_116
ExportToSpreadsheet	Select or enter the column Export all measurements	Tab True
ExportToDatabase	Database type DatabaseName User name & password	MySql Db_ HCT_116 Enter your own user name & password

4.3.7 Database

MySql 5.1 open source database was used to store the information after processing images.

4.3.8 Programming language

The stored data is analyzed by developing graphs of different variables with help of Matlab 7.9.0.

5. RESULTS

5.1 Proteasome Inhibition by Bortezomib

Algorithmic pipelines as shown in table 1 and table 2 were able to successfully process the images of MelJuSo-Ub cell line treated with Bortezomib. Fluorescent signal was captured by means of the image processing algorithms employed, showing increase and decrease in proteasome inhibition just after the treatment of cell line with Bortezomib. When the number of fluorescent spots (cells) were plotted as a function of time it revealed a rapid increase in the number of fluorescence spots on the image that reached to its peak after 10 hrs of treatment where after for next 10 more hours they kept on increasing but their rate of increase become quite slow. At 20th hr a sharp decrease was observed till next 20 hrs as shown in fig 2. While in the remaining 32 hrs a very few cells (~10) emitted the fluorescent.

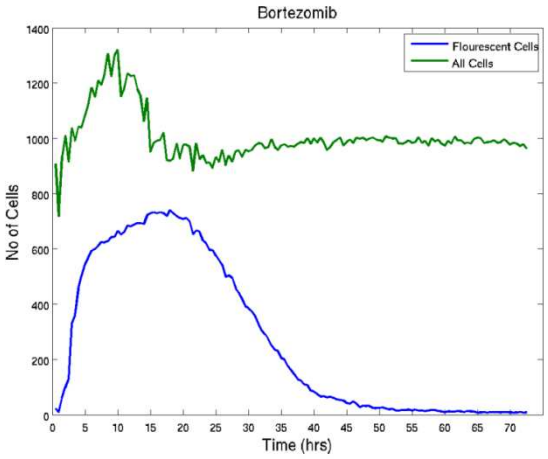

Fig 2. Number of cells emitting fluorescent signal upon treatment with Bortezomib.

5.2 Proteasome inhibition by CB3

CB3 is also a proteasome inhibitor and the number of colored spots reaches quickly to its maximum (~ 500) at 6hr after treatment with CB3. This is reflected by the very steep initial part of the blue curve in fig. 3.The curve then became approximately constant for the next 10 hrs. After this time interval, there is a continuous decline in the fluorescent cells until end of experiment (72 hrs). Control (untreated) cells of the MelJuSo-Ub were also monitored up to 72hrs, and the numbers of cells that showed the fluorescent signal were very scarce (145 total, ~ 2 per hr) as shown in fig 4.

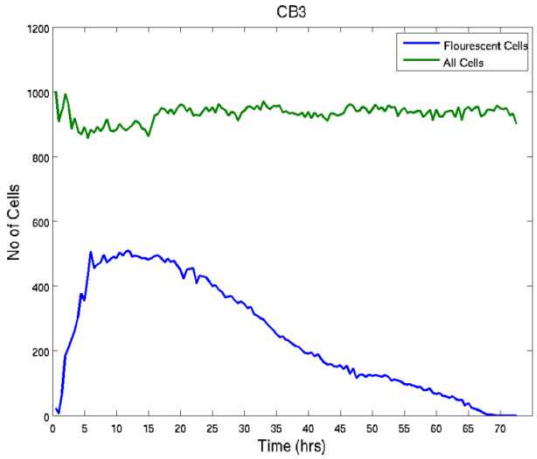

Fig 3. No of cells emitting fluorescent signal after treatment with CB3.

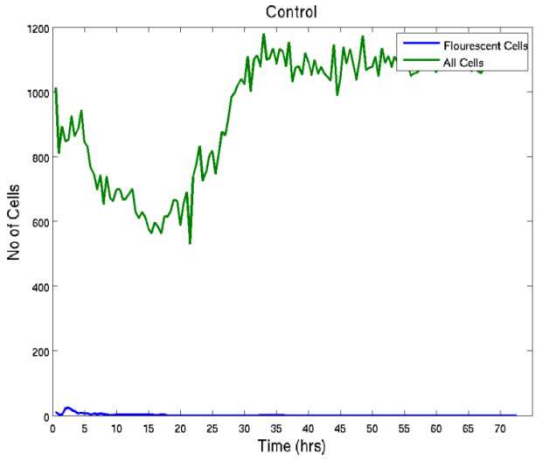

Fig 4. No of untreated cells emitting fluorescent signal.

5.3 Comparison of proteasome inhibition with Bortezomib and CB3

Fluorescent microscopic images of both Bortezomib and CB3 were processed by using the same pipeline described in table 1. The algorithms were sensitive enough to read the fluorescent signals as small as few pixels from both set of images. Bortezomib inhibited proteasome at the maximum ~ 730 cell while CB3 number remained at ~500. Bortezomib rate of inhibition of cells (273 per hr) was higher than the CB3 (242 per hr). The number of cells inhibited by Bortezomib was kept on increasing for 20hrs after treatment. While in case of CB3, number of inhibited cells was increased up to 6hrs and after that for next 10 hrs number of cells stabilizes (fig. 5). This stabilization of inhibition is unique to CB3 because number of inhibited cells decreased rapidly after the maximum point had reached in case of Bortezomib. Towards the end another contrast becomes apparent because number of inhibited cells by CB3 showed gradual reduction of fluorescent spots with passage of time. It forms a continuous steep while Bortezomib produces a sharp steep and then stabilizes at about 50 hrs.

The percentage of cells that were inhibited at the maximum point by the Bortezomib was 80% as compare to CB3 which inhibited 57% (fig. 6). During first 12hrs the % effect of both drugs on the proteasome inhibition was almost similar. Then % effect of the CB3 starts decreasing gradually until 72th hr while Bortezomib improved % effect for next 6 hrs (total 18hr) and from where it steeps down to 2% inhibition at the 50^{th} hr as comparison to CB3 which attain the same inhibition at the 67^{th} hr.

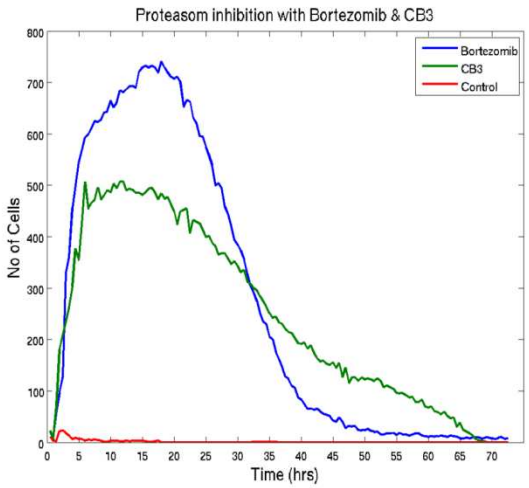

Fig 5. Comparison, number of cells under proteosome inhibition with Bortezomib and CB3.

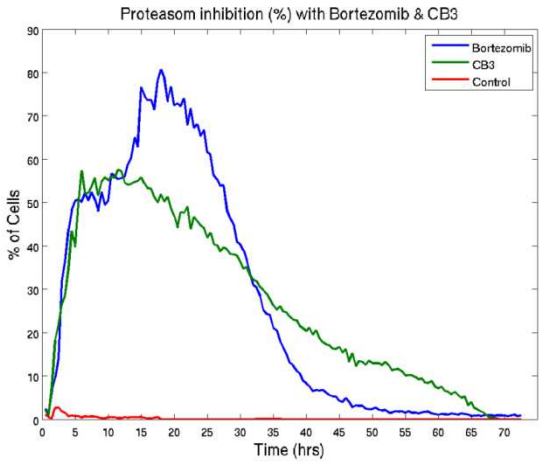

Fig 6. Comparison, percentage (%) of cells under proteosome inhibition with Bortezomib and CB3.

Intensity of the fluorescent signal was to measure how colored a signal was after treatment with the proteasomal inhibitor. Algorithmic pipeline calculated the intensities of the fluorescent signal and their plot showed, those images that were captured after treatment of Bortezomib were more colored as compare to the CB3 (fig 7). Fluorescent images of the control also showed a quite sharp signal at the random places that was due to the bad quality of these images.

Time lapsed images of Bortezomib gradually increased to the highest intensity value during first half (31hrs) of experiment and then decreases gradually in the second half of the experiment. While CB3 obtained its maximum fluorescence peak (far less than Bortezomib) in 22 hr and then approximately sustain it until end of experiment.

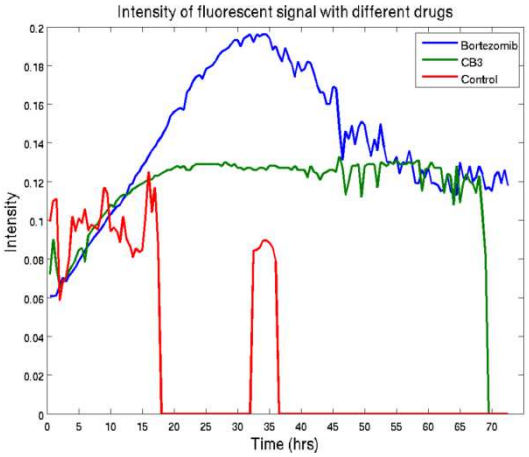

Fig 7. Intensity fluorescent signals of images taken after treatment with Bortezomib, CB3 and control.

5.4 Cell Clumps (spheroid) of hTERT RPE-1 Cells

Time lapsed microscopic images of the hTRET RPE-1 had strong background noise and it was hard to extract features from these images. A Gaussian filter was applied to these images and resulting images were processed with algorithmic pipeline as described in table 4.

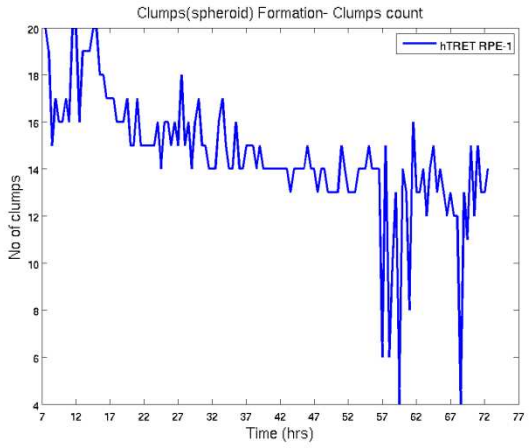

Fig 8.A. No. of cell clumps in each time lapsed microscopic image.

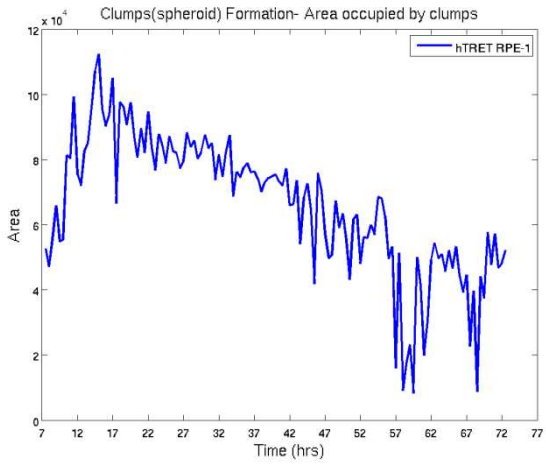

Fig 8.B. Area (pixels) occupied by clumps in each time lapsed microscopic image.

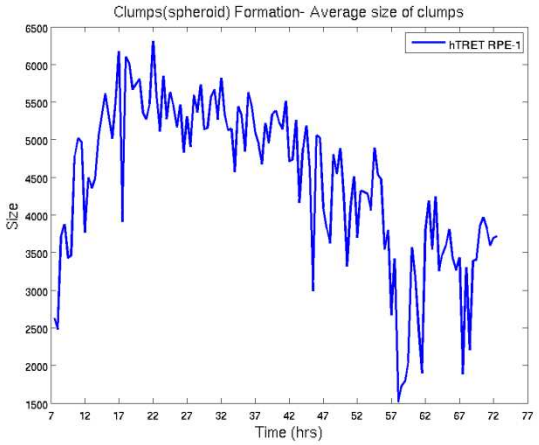

Fig 8.C. Average size (area occupied/no. of clumps) of cell clumps.

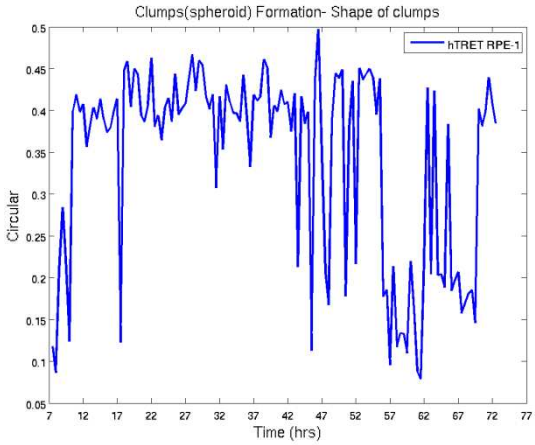

Fig 8.D.Measure of form factor (roundness) of cell clumps formed by hTRET RPE-1.

Cells organized to form spheroids after ~6 hrs of their growth on the nanoculture plates. Before this cells were more like scattered spots on microscopic images. It is evident from fig 8 A, that number of the clumps (20 clumps) in the start was more as compare to the end (14 clumps) of the experiment. As time passed more and more cells joined the spheroids so area occupied (fig 8. B) by the spheroids decreased from 20hrs to 72hrs(fig. 8.G).Spheroid formation was also shown (fig 8. C) where average size of the spheroids was calculated.

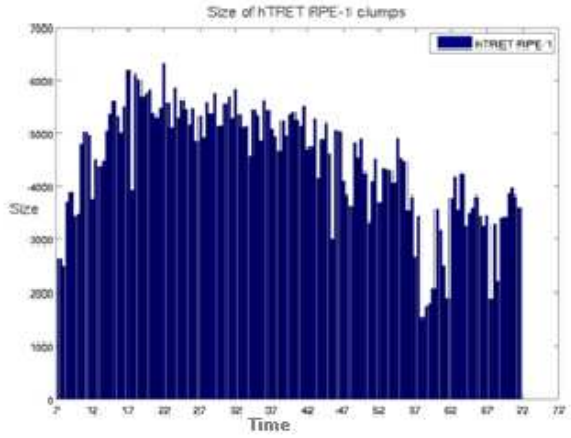

Fig 8.G. Size of clumps of hTRET RPE-1.

Average size was 5500 pixels during 15 to 20 hrs when the spheroid formation was in process. This also correspond to fig 8. A and fig 8.B where number of spheroids were highest, and area occupied by them was also at peak during this duration of time. A consistent decline was observed after 20 hrs in the average size of the clumps till 72 hrs. The shape of the spheroids was clumsy at the start of experiment but from 7 hr they started to organize in the round shape with the joining of more and more cells up to 17 hrs (fig 8. D). At this time point they obtain their maximum round shape and almost sustain this shape till the end 72 hrs of the experiment.

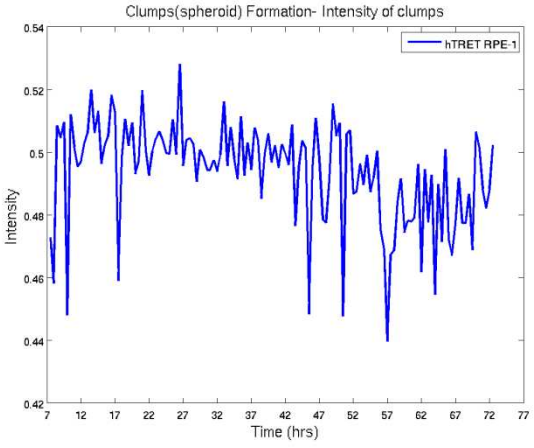

Fig 8.E.Measure of Intensity of cell clumps formed by hTRET RPE-1.

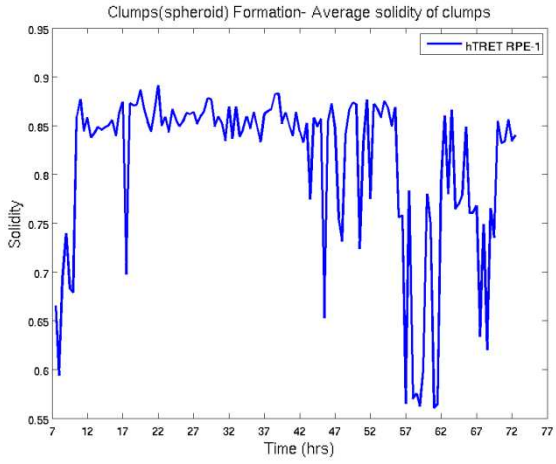

Fig 8.F.Measure of solidity (convexity) of cell clumps formed by hTRET RPE-1.

The intensity of the spheroids was quite consistent except 54 to 73 hrs when they show a gradual decrease in the intensity as shown in fig 8.E. Solidity is the measure of convexity of an object. Spheroids were quite solid from 12 to 55 hrs after that they showed a decrease in their solidity (fig 8. F).

5.5 Cell Clumps of HCT 116 Cells

Images of cell clumps from the time lapsed microscopy was obtained after the growth of HCT 116 cell lines in Incucyte^{TM} for 72 hours. These images were then processed at two stages in order to extract meaningful information. At the first stage a Gaussian filter was applied that made the

images smoother. These semi-processed images were processed by using the pipeline described in the table 5. Some of the phenotypic characteristics of these cell clumps are shown below fig 9 A-F.

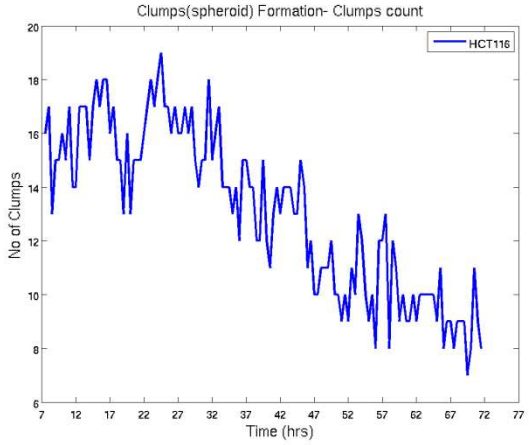

Fig 9.A.Cell clumps count in each time lapsed microscopic image formed by HCT 116.

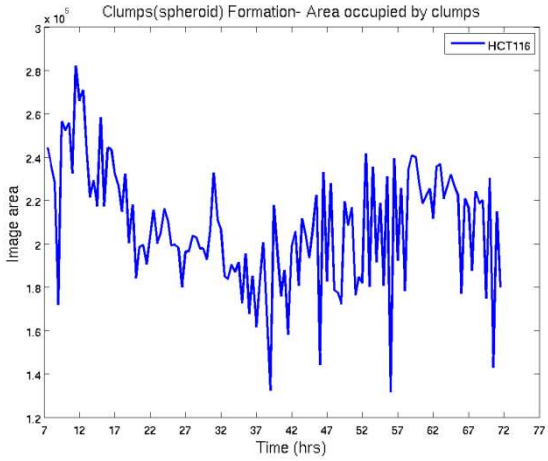

Fig 9.B. Area (pixels) occupied in each image by cell clumps.

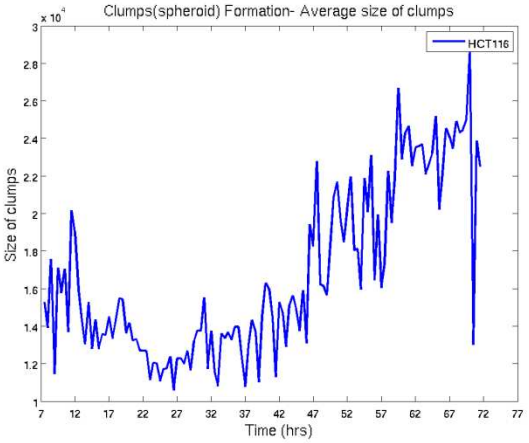

Fig 9.C. Cell clumps average size (area occupied/no. of clumps).

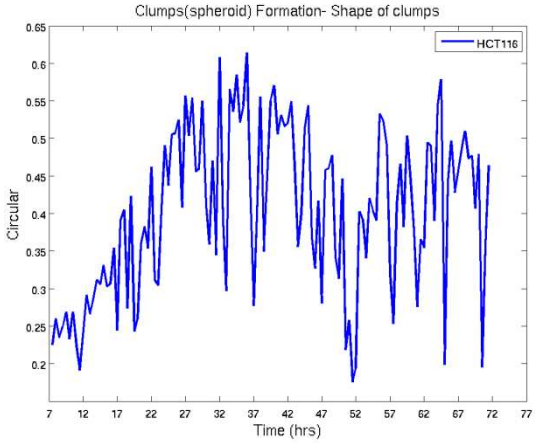

Fig 9.D. Measure of form factor (roundness) of cell clumps formed by HCT 116.

Cells were in the haphazard shape in the first 6 hrs of the experiment but from ~7 hrs they started organizing into spheroids. This organizing process continued till 25hrs as shown in fig 9.A. Number of clumps increased in the beginning 7 to 25 hrs after that there was a continuous steep in the reduction of number clumps. The continuous reduction may be due to the fact that some smaller clumps may have joined the larger ones. This may also be interpreted from fig 9. B &C, where sizes of the spheroids keep on increasing (fig 9.G) while the total area under the spheroids decreased at the same time.

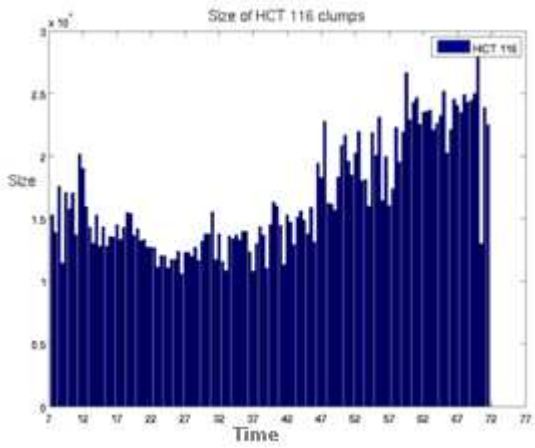

Fig 9.G. Size of clumps as a function of time.

Total area covered by spheroids on each time lapsed image is shown in Fig 9.B. Total area of the spheroids decreased from $2.8x10^5$ to $1.9x10^5$ during 11 to 38 hrs respectively. It then showed increase in the occupied area till 60 hrs. From 7 to 27 hrs the average size of the spheroids was decreased because clumps were in still organizing process as also shown in fig 9.A. After the 27 hrs average size of clumps showed a steady increase until end of experiment. The clumps were in some irregular shape at the start of experiment and there was a trend to form the circular shape up to 30 hrs shown in fig 9 D. This also strengthened that cells were organizing to form spheroids during that time period. Then cells showed a slight decrease towards spherical shape trend up to end of experiment.

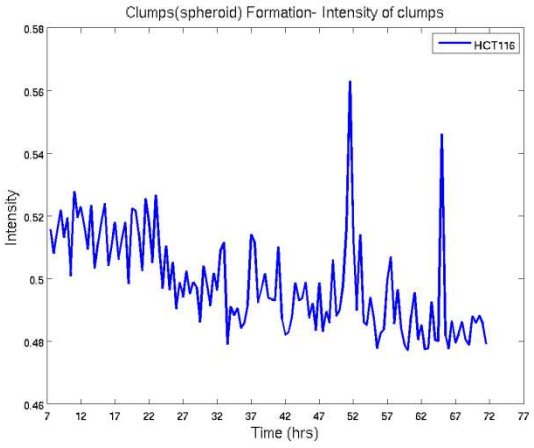

Fig 9.E. Intensity of cell clumps formed by HCT 116.

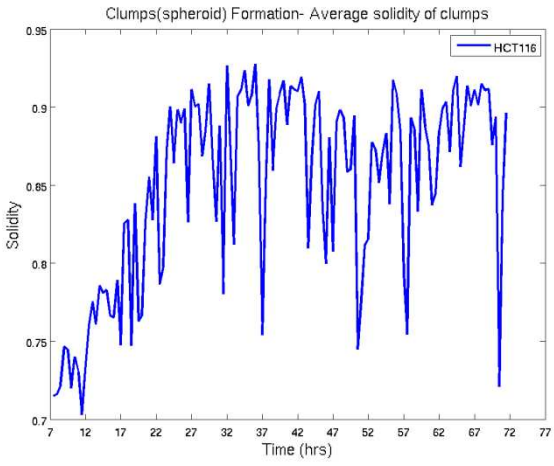

Fig 9.F. Clumps HCT 116, solidity (convexity).

Graph of intensity of cell clumps in this experiment is shown in fig 9.E. Cell clumps showed a gradual decrease in the intensity with the passage of time. On the other hand solidity fig 9. F of spheroids was less at the start of experiments but it kept increasing up to 27 hrs when cells were quite organized in to clumps. During the 27 to 72 hrs cell clumps solidity was more or less remained same.

5.6 Comparison of cell clumps formation in both experiments

Cell clumps formed by hTRET RPE-1 were small in size as compare to the cell clumps formed by HCT 116 (fig 10.C), that made it obvious that the number (1902 total) of hTRET RPE-1 cell clumps may be more as compare (1690 total) to HCT cell clumps (fig 10.A).There is similar trend of decrease of the number of clumps as the time passes in the experiment. Size of HCT 116 cell clumps keep on increasing towards the end of experiment while the size of hTRET RPE-1 cell clumps decreases at the same time.

Both cell lines obtained their maximum number and maximum area of image under clumps at almost same time 14-17 hrs (fig 10.A &B).The area of image under HCT 116 clumps is about 4 times as compare to the clumps of hTRET RPE-1. Both cell lines have the tendency toward round shape formation fig 10 D. However cell clumps formed by HCT 116 were more rounded in shape as compare to the hTRET RPE-1 cell clumps. HCT 116 cell clumps obtain their maximum roundness (~.62 form factor) at 36 hr as compare to hTRET RPE-1 cell clumps, which obtain maximum roundness (~.48 form factor) at 28 hr. After obtaining maximum organization in shape both cell lines have the tendency of slow degradation in shape.

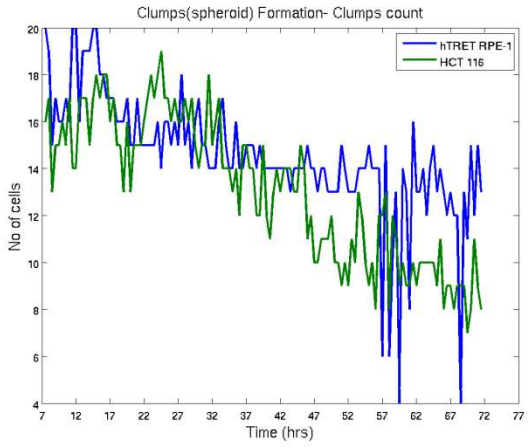

Fig 10.A.Comparison of no. of cells in each time lapsed microscopic image formed by hTRET RPE-1 and HCT 116.

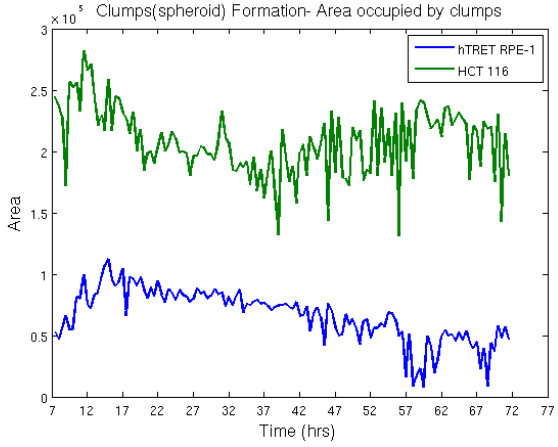

Fig 10.B.Calculation of area (pixels) occupied in each image by both types of cell clumps.

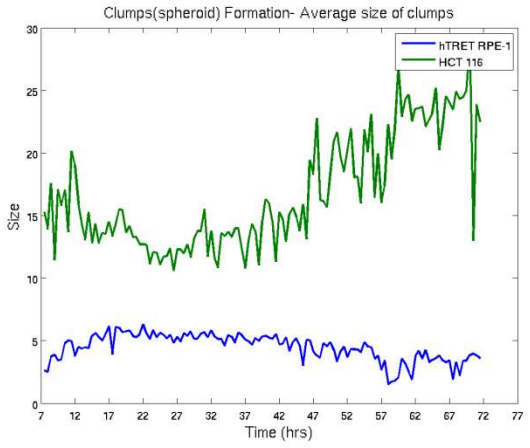

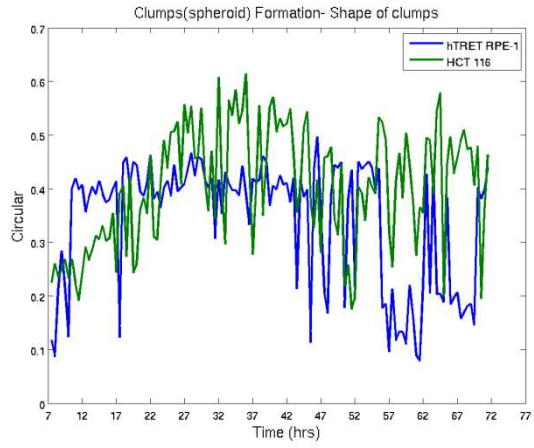

Fig 10.C. Comparison of spheroid's average size (area occupied/no. of clumps).

Fig 10.D. Comparison. Shape (roundness) of cell clumps.

Cell clumps of both cell lines showed almost same intensity fig 10.E. It may be due to the treatment of images of both cell lines with Gaussian filter. However, the solidity (convexity) showed similar trend of increase in the start of experiment. But this trend is abrupt in hTRET HPE-1 while it is gradual in case of the HCT 116. Both cell lines again showed the similarity in convexity by showing decrease in the convexity towards the very end of experiment.

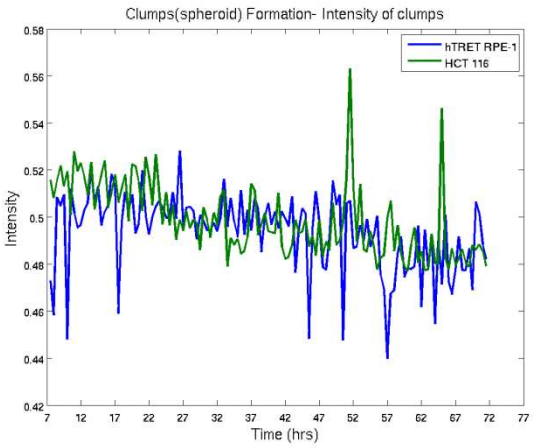

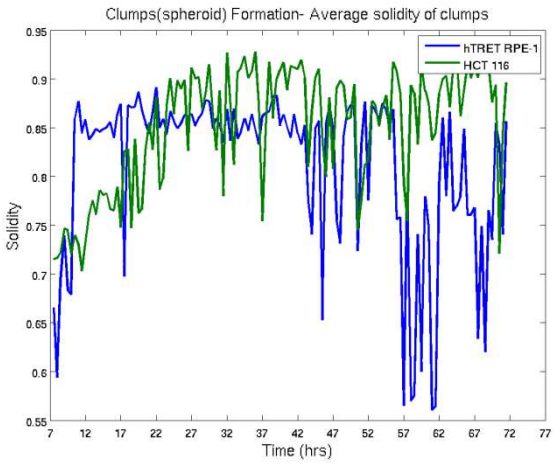

Fig 10.E. Intensity of cell clumps formed by hTRET RPE-1 &HCT 116.

Fig 10.F. Comparison of solidity (convexity) of cell clumps.

6. DISCUSSION AND SUGGESTIONS FOR FUTURE WORK

In this thesis, a novel bioinformatic infrastructure has been proposed, implemented and demonstrated to extract novel types of kinetic information about cell population dynamics. Using the open source software CellProfiler, by combining various modules into pipelines, along with the proper parameters (at some time external pre processing), the results presented show that one can effectively extract valuable phenotypic information from the phase contrast as well as fluorescent microscopic images.

This study consisted of two biomedical studies; in the first part proteasome inhibition of MelJuSo-Ub cell line was studied with Bortezomib and a novel protesome inhibition hit CB3. While in the second study cell clumps (spheroid) formation of HCT 116 and hTRET RPE-1 cell lines was monitored when grown on the novel cell growth plates (nanoculture plates having honeycomb film at base).

6.1 Proteasome Inhibition

It is evident from this study that Bortezomib is more effective for proteasome inhibition in MelJuSo-UB cell lines than CB3 (fig.5), Bortezomib showed 35001 fluorescent spots as compare to CB3 (25420) in first 32 hrs. Fluorescent signals were more sharp incase of Bortezomib time lapsed microscopic images. It was due to fact that more molecules were exhibiting fluorescence than CB3 images (fig. 7). Activity of Bortezomib is consistent with the studies [42] [43][45] that

showed it has effective proteasome inhibition activity and is first drug being used in clinical trials for treatment of cancer.

This study can easily lead to ascertain the time when drugs have their optimum effect on cells. In our case Bortezomib and CB3 both showed the high fluorescent signals at 15 hour after treatment (fig 5). Duration of effect is large in case of CB3 (Number of fluorescent cells decreased to 10% in 55hrs as compare to 39hrs for Bortezomib); it means CB3 effect the proteasome inhibition slowly but at the long time span as compare to Bortezomib (fig 5).This is an important property because in some cases duration of drug activity is important for treatment [46].Prolonged proteasome inhibition cause the toxicity by accumulating deleterious proteins [44] therefore duration of drug effect is important to calculate interval after which another dose of drug may be administered, indeed role of other aspects such as half life also needed to take into account before deciding dose interval.

The work showed the improved way to achieve the work done by Rickardsonet al [36] in the sense that images were taken from Incucyte^{TM} and IncucyteFLR and it was demonstrated that open source software can process the images from both sources in contrast to former where array scan fluorescent images were used with cellomic software. Proteasome inhibition studies as [36] lacks kinetic aspect of drugs, time lapsed microscopic based image processing algorithms provided in this study were helpful in detailed study of the proteasome inhibitors such as Bortezomib and CB3 up to 72 hrs and sampling at every half hour. Efficacy and phenotypic effects of CB3 and Bortezomib can be studied along time scale that could be helpful in drug discovery.

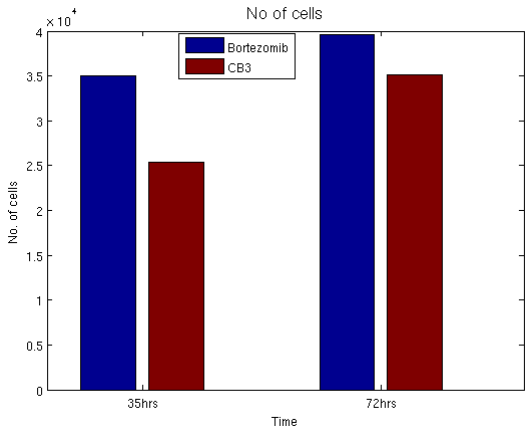

Fig 11. Number of fluorescent cells after 35 and 72 hrs treatment with Bortezomib and CB3.

Total number of fluorescent cells (fig. 11) produced after treatment with Bortezomib were39593 as compare to CB3 35124 having %11difference in number of inhibited cells when calculated as function of time. This is interesting result because it shows that Bortezomib effects fast (27% more in first 35hrs) but the number of inhibited cells are more close to number of cells inhibited by CB3 at the end. Therefore it may be deduced that both have very close efficiency in terms of inhibition of cells. But further studies are required to be conducted to evaluate it because it might be possible that Bortezomib may have inhibited all cancerous cells present in focus of view of the microscope.

6.2 Cell Clumps (spheroid) Formation

Cell clump studies are gaining momentum because cancerous cells can grow in the form of clumps inside body therefore the effect of the drugs on clumps may be different in comparison with unnatural monolayer flat cell cultures [41]. The study provides the very novel arrangements of algorithms that can not only identify the clumps and extract their phenotypic details but successfully exclude the back ground noise produced in images by nanoculture plate structure.
Nanoculture plates have honeycomb structure; therefore time lapse microscopic images of cell clumps had background noise that makes them hard to be identified. A Gaussian filter was used to suppress background noise in these images.

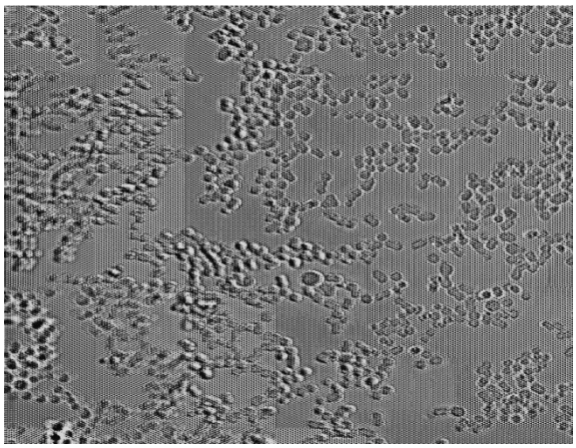

Fig 12.A.HCT 116 cells after 1 hr of growth.

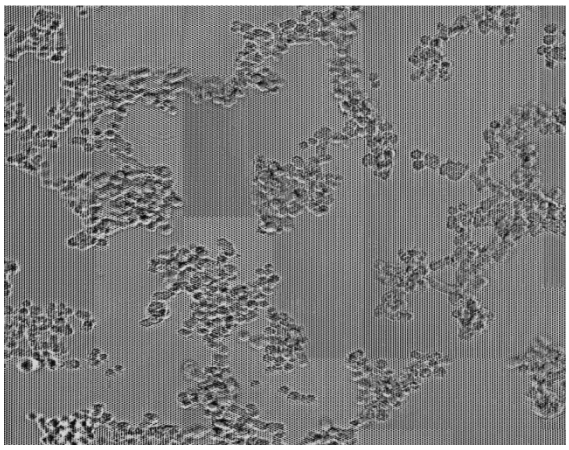

Fig 12.B. HCT 116 cells after 7 hr of growth.

This study showed that both hTRET RPE-1 and HCT 116 cell lines can form cell clumps. Therefore drugs can be tested for their permeability and sensitivity because clumps are supposed to create tumor micro environment [48]; and understanding of cellular behavior in culture and in vivo will also be increased [47]. There was a tendency of HCT 116 cell line to form large clumps as compare to other one (fig. 13 &fig 10.C). Penetration of most drugs in spheroids is size dependent and face difficulty in penetration therefore outer cells of clumps have larger concentration of drugs [49]. So it can be assumed that HCT 116 cell clumps may be more resistant to drugs as compare to hTRET RPE-1 cell clumps.

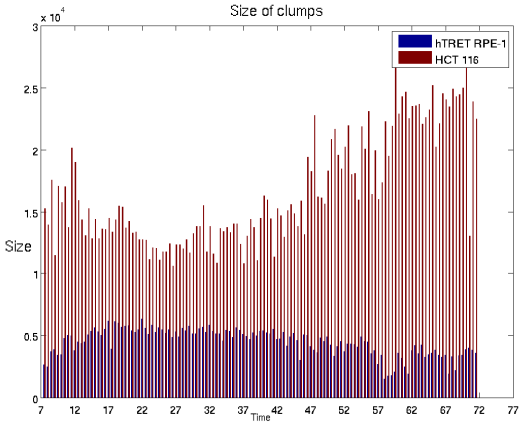

Fig 13. Comparison of sizes of clumps.

Both cell lines on the honeycumb structure can take, up to 6-7 hrs, for initial arrangements (fig. 12.A&B) that then can lead to fully distinguishable spheroids. Spheroid of both cell lines also showed the tendency to form the circular shape where first 17 hrs for hTRET RPE-1 and first 32 hrs were important for HCT 116 in this regard (Fig.10.D.). Growth and then resulting shape of clumps is highly dependent on the geometry of the pattern of the nanoculture plates [41].

Spheroids of HCT 116 were reduced in number (fig 10.A.) towards the end of experiment and their sizes were increasing at the same time. It was due to fact that whenever a clump came close to another one they combine to form a larger clump. Structure became quite stable after 20 hr when drugs can be added to study their permeability and sensitivity in cell clumps. It is also noted without any drug these structures are quite stable even after 72 hrs.

Multiparametric assays of phenotype can also help us to understand details about biology involved in the process and let us predict to gene involved [37] for specific phenotype. In [37] the phenotypic effect of genes on mitosis was studied. Which shows it is possible to predict gene if we know the phenotypic profiling of the cells. Similarly large size and more round shape clumps tell us that there are more tendencies of HCT 116 cells to form the clumps and that gene/ genes involved in clumps formation is more active in HCT 116 than hTRET RPE-1. Phenotypic studies can also tell us about the phenomenon or the study of cell cycle as in [39 and 40].

6.3 Suggestions for future work

Assays of proteasome inhibition and cell clumps formation were performed on small scale; success of them showed that such type of assays can be conducted on the large scale for fluorescent based analysis or phenotypic profiling of chemical libraries [38]. Cell clumps experiments were also test experiments to test the growth of clumps on the nanoculture plates. Now drugs based cell clumps assays could be initiated to study cancer [50] and effects of drug in the almost similar to in vivo conditions.

Never the less these assays can be improved by tracing objects (space) as a function of time. Such type of spatiotemporal studies will open provide new exiting information [40]

Phenotypic profiling of the human genome [37] using multi-parametric phenotypic assays provides a rich dataset for scoring phenotypes and then predicting the gene involved.

Phenotypic profiling assays can also predict the ligand target interaction [38] which is very important information for early drug discovery. This is another dimension where current study can also be extended.

ACKNOWLEDGEMENTS

I would like to acknowledge my supervisor Prof. Mats Gustafsson, for his continuous support in my MS project. He helped me a lot in my research, provided supportive environment, encouragement, and was always there to listen and to give advice promptly, making me able to complete this report. I would like to express my gratitude to my co-supervisor Dr. Erik Bongcam for solving lot of problems.

Special thanks go to Prof. Rolf Larsson and Dr. Marten Fryknas for their support and providing valuable research material. Great help was also provided by Dr. Claes Andersson and M.Sc Christofer Backlin. I am also grateful to HEC for their support.

I also like to thank my friends especially Obaid Aftab, Awaisa Ghazal and all others who encourage and helped me.

REFERENCES

[1] Zernike F., Groningen: "Phase contrast, A new method for microscopic observation of transparent objects", Part 1, (1942), Physcia IX, no. 7, 686-698.
[2] Zernike F., Groningen: "Phase contrast, A new method for microscopic observation of transparent objects", Part II, (1942), Physcia IX, no. 10, 974-986.
[3] http://www.microscopy-uk.org.uk/index.html, seen as at 2010-05-16.
[4] Frederick C. Grigg: "Colour-contrast phase microscopy", (1950), Nature 165.
[5] Vonesch C., Aguet F., Vonesch J. and Unser M: "The colored revolution of bioimaging", (2006), IEEE signal processing magazine. 20-31.
[6] Masters, Barry R: "The development of fluorescence microscopy", (2010), Encyclopedia of life sciences. John Wiley & Sons, Ltd: Chichester, DOI:10.1002/9780470015902.a0022093.
[7] *Haugland, R.P. et al:* "Introduction to fluorescence microscopy in Handbook of fluorescent probes and research products", (2006), Moleculer probes, Inc, Eugene, Oregon, 1-6.
[8] Shimomura O., jhonson F.: "Extraction, purification and properties of aequorin, a bioluminescent protein from luminous hydromedusan, Aequorea", (1962), Cell Comp Physol.59: 223-39.
[9] Chalfle M., Tuy, Euskirchen G.: "Green fluorescent protein as a marker for gene expression",(1994), Science, 263(5148): 802-5.
[10] http://www.essenbioscience.com, seen as at 2010-05-16.
[11] Kankaanpaa P. et al: "BioImageXD- New open source free software for processing, analysis and visualization of multidimensional microscopic images", (2006), Microscopy Today, 12-16.
[12] Collins T. J.:"ImageJ for microscopy",(2007), Imaging Forentires, Vol. 43, 25-29.
[13] Carpenter A.: Thouis R Jones et al: "CellProfiler: Image analysis software for identifying and quantifying cell phenotypes",(2006),Genome Biology,Vol. 7, Issue 10, Article R100.
[14] http://www.broadinstitute.org/science/software, seen as at 2010-05-20.
[15] http://www.cellprofiler.org, seen as at 2010-05-20.
[16]http://www.worldlingo.com/ma/enwiki/en/High-content_screening#High_Content_Screening.E2.8094a_definition , seen as at 2010-05-25.
[17] Coons, A.H. and Kaplan, M.M: "Localization of antigen in tissue cells.II. Improvements in a method for detection of antigen by means of fluorescence antibody", (1950), J.Exper.Med.Vol.91 no.1: 1-13.
[18] D. Lansing Taylor: "Past, present and future of high content screening and filed of cellomics", (2006), Methods in Molecular Biology.Vol. 356, humana Press, Inc., Totowa, NJ, 1-16.
[19] Ingram, M. and Preston, K., Jr.: "Automatic analysis of blood cells.", (1964), Scientific Amer, 223,72.
[20] Castleman, K. R.: "Digital Image Processing." (1979), Prentice-Hall, New Jersey.
[21] Prewitt, J. M. S. and Mendelson, M. L.: "The analysis of cell images.", (1966), Ann. NY. Acad. Sci. 128, 1035.

[22] Taylor, D. L. and Wang, Y. -L. (eds.): "Fluorescence microscopy of living cells in culture. Parts A and B, in Methods in Cell Biology", (1989), Academic, New York, 29-30.
[23] Korn K. and Krausz E.: "Cell-based high content screening of small molecule libraries",(2007), Current opinion in chemical biology, Elsevier, 11: 503-510.
[24] Yu ksel, M. E.: "Edge detection in noisy images by neuro-fuzzy processing", (2007), International journal of electronics and communications 61(2), 82-89.
[25] Alper Bas tu rk a, Enis Gu nay: "Effective edge detection in digital images using a cellular neural network optimized by differential evolution algorithm", (2009), Experts systems with applications 36(2009), 2645-2650.
[26] Weihua wang: "Reach on Sobel operator for vehicle recognition", (2009), 2009International joint conference on Artificial intelligence, IEEE computer society, 2009.54, 448-450.
[27] Abbasi T. and Abbasi M.: "A novel architecture for Prewitt edge detector", (2009), Journal of active and passive electronic devices, Vol. 8, 203-211.
[28] Canny J.: "A computational approach to edge detection", (1986), Transaction on pattern analysis and machine intelligence, Vol. PAMI-8, no. 6. IEEE, 679-680.
[29] Soo-Chang pei, Ji-Hwei Horng: "Design of FIR bilevel Laplacian of Gaussian filter",(2001), Signal processing 82(2002) Elsevier, 677-691.
[30] Bruk J. and Pw Sternberg: "An automated system for measuring parameters of nematode sinusoidal movement", (2005), BMC Genetics, 6:5.
[31] Otsu N.: "A threshold selection method from gray level histograms", (1979), Transaction on systems, MAN and cybernetics, Vol.SMC-9, no.1, IEEE, 62-64.
[32] http://www.qi.tnw.tudelft.nl/Courses/FIP/frames/fip-Sigmenta.html, seen as at 2010-05-25.
[33] khashman A. Sekeroglu B.: "A novel thresholding method for text separation and document enhancement", 11th panhellenic conference in informatics, 323-330.
[34] Rajendran N. Sid-ahmed and Soltis J.J: "Multilevel thresholding and its application to feature extraction in machine parts", 1984, IEEE, 32.8.1-32.8.4.
[35] http://micro.magnet.fsu.edu/primer/java/digitalimaging/processing/diffgaussians/ index.html, seen as at 2010-05-25.
[36] Rickardson L., Wickstrom M., Larsson R. and Lovborg H.: "Image-based screening for identification of novel proteasome inhibitors", (2007), Journal of biomoleculer screening 12(X): 1-8.
[37] Beate Neumann et al: "Phenotypic profiling of human genome by time-lapse microscopy reveals cell division genes", (2010), Nature, Vol. 464, 721-727.
[38] Young W. D. et al: "Integrating high content sceerning and ligand-target prediction to identify mechanism of action", (2008), Nature chemical biology.Vol.4, no.1, 59-67.
[39] Haseyama M. and Sasamura Y.: "Effective apoptotic cell extraction from video microscopy images", (2005), IEEE, II-461- II-464.
[40] Kang Li et al: "Cell population tracking and lineage construction with spatiotemporal context",(2008), Medical image analysis, Elsevier, 546-566.
[41] http://www.infinitebio.com/ibi2/products/scivax-3d-culture/index.htm, seen as at 2010-05-20.
[42] Adams J. et al: "Development of the prteasome inhibitor Velcade™ (Bortezomib), (2004), Cancer Investigation, Vol 2, no.2, 304-309.
[43] Caravita T. et al: "Bortezomib: efficacy comparison in solid tumors and hematologic malignancies", (2006), Nature reviews clinical oncology 3, 374-387.
[44] Ding Q., Dimayuga E., William R. Markesbery and Jeffrey N. Keller: "Proteasome inhibition induces reversible impairments in protein synthesis", (2006), FASEB Journal, 1055-1063.

[45] Wee J.Chng et al: "Molecular dissection of hyperdiploid multiple myeloma by gene expression profiling", (2007), Cancer research 2007, 67(7), 2982-2989.
[46] Mathias R.: "Rate and duration of drug activity play major roles in drug abuse, addiction and treatment", 1997, NIDA Vol.12, no.2.
[47] Justice A., Nadia A. Badr and Felder A.: "3D cell culture opens new dimensions in cell based assays", (2009), Drug discover today, Elsevier,Vol. 14, no. 1/2, 102-107.
[48] Roncoroni L. et al: "Cytogenetic characterization and cell cycle analysis of three human colon adenocarcinoma cell lines: Comparison between two and three dimensional cell culture systems",(2010), Cancer Investigation, 28:7-12.
[49] Sutherland M. R: "Cell and environment interactions in tumor microregions: The multicell spheroid model", (1988), Science, Vol. 240, issue 4849, 177-184.
[50] Frieboes B. H. et al: "Prediction of drug response in breast cancer using integrative experimenta/computational modeling", 2009, Cancer Res 2009, 69(10), 4484-4492.
[51] Wilson D. G.: "Cell kinetic studies using a monoclonal antibody to Bromodeoxyuridine", (2nd edition), Methods in molecular biology, Vol. (80), 255-265.